Niclosamide methanol solvate and niclosamide hydrate: structure, solvent inclusion mode and implications for properties

Authors

Bethany I. Harriss[a], Claire Wilson[b] and Ivana Radosavljevic Evans[a]*

[a]Department of Chemistry, Durham University, Durham, DH1 3LE, United Kingdom

[b] Diamond Light Source, Didcot, OX11 0DE, United Kingdom

Correspondence email: ivana.radosavljevic@durham.ac.uk

Synopsis Niclosamide methanol solvate forms a crystal structure with continuous channels along the crystallographic a-axis, providing a pathway for the removal of the solvent molecules.

Abstract We have carried out structural studies of two solid forms of niclosamide (5-chloro-N-(2-chloro-4-nitrophenyl)-2-hydroxybenzamide, NCL), a widely used anthelmintic drug, niclosamide methanol solvate and niclosamide monohydrate H_A. The methanol solvate structure obtained from single crystal X-ray diffraction is reported for the first time, elucidating the key hydrogen bonding host-guest interactions which lead to solvate formation. The essentially planar niclosamide host molecules interact via π-stacking and pack in a herringbone-type arrangement, giving rise to channels along the crystallographic *a*-axis in which the methanol guest molecules are located. The methanol and niclosamide molecules interact via short O-H•••O hydrogen bonds. Laboratory powder X-ray diffraction demonstrates that initially phase-pure niclosamide methanol solvate readily transforms into niclosamide monohydrate within hours at ambient conditions. PXRD further suggests that niclosamide monohydrate H_A is isostructural with the NCL-MeOH solvate. This is consistent with the facile transformation of the methanol solvate into hydrate when stored in air. The crystal packing and topology of guest molecule inclusion is compared to that of other niclosamide solvates whose crystal structures are known, giving a consistent picture which correlates well with known experimentally observed desolvation properties.

1. Introduction

Niclosamide (5-chloro-N-(2-chloro-4-nitrophenyl)-2-hydroxybenzamide, hereinafter abbreviated NCL) is an anthelmintic drug which has been marketed for many years to treat tapeworm infestations. (Sanphui *et al.*, 2012, Weinbach & Garbus, 1969) Very recently, it has also been investigated for additional therapeutic applications, including anti-bacterial and anti-tumor activities.(Helfman, 2011, Imperi *et al.*, 2013, Yo *et al.*, 2012) NCL is a BCS class II drug, virtually insoluble in water, and is

formulated as a suspension and in chewable tablet form. Although both NCL anhydrate and monohydrate are available for drug formulation, each has drawbacks; the high affinity of the anhydrate for water and the poorer solubility of the hydrate can cause sedimentation during storage. (van Tonder, Maleka*, et al.*, 2004) NCL contains multiple potential hydrogen bonding sites (NO_2, OH and carbonyl groups) and two Cl atoms which could form halogen bonds (Fig. 1). Generally, these structural features favour formation of solvates and cocrystals, which represent, in principle, viable methods for improving the solubility and reducing the hygroscopicity of NCL.

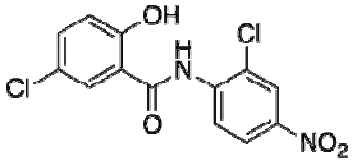

Figure 1 Chemical structure of niclosamide.

The anhydrous form of NCL is prone to solvate and hydrate formation. The structure of guest-free niclosamide is built up by the essentially planar molecules interacting via moderate (Steiner, 2002) O-H···O hydrogen bonds (d_{OO} = 2.69 Å), weak Cl···NO_2 interactions (d_{ClO} = 3.22 Å) and π-stacking (with 3.33 Å separation between planes and 3.74 Å separation between ring centroids). (Sanphui *et al.*, 2012) Several solvates, with methanol, dimethyl sulfoxide, dimethylformide, diethyl ether, tetrahydrofuran (THF) and tetraethylene glycol (TEG), have been identified. (Caira *et al.*, 1998, van Tonder, Mahlatji*, et al.*, 2004, van Tonder, Maleka*, et al.*, 2004) However, only the crystal structures of the tetrahydrofuran and tetraethylene glycol solvates have been determined.

Two niclosamide monohydrates (H_A and H_B) have been identified and the structure of H_B has been determined from single crystal diffraction data. (Caira *et al.*, 1998) This showed the water molecules confined, in pairs, into closed cavities in the structure, accounting for the high temperature of the onset of dehydration (173^{o}C). The structure of the monohydrate H_A remained unknown, although its significantly lower dehydration temperature (100^{o}C) suggested that the water molecules inclusion mode was substantially different from that in H_B. The relationship between the two niclosamide monohydrates was studied further by a range of methods, which consistently suggest that H_A is the kinetically favoured form which readily transforms into H_B. (Manek & Kolling, 2004, Tian *et al.*, 2010, van Tonder, Mahlatji*, et al.*, 2004)

Physical property measurements reported on the solvates listed above, including solubility, dissolution and thermal properties, revealed a high affinity for water of all these crystal forms. (van Tonder, Mahlatji*, et al.*, 2004, van Tonder, Maleka*, et al.*, 2004) This may have potentially impacted some of the measurements reported, given that, for example, niclosamide tetrahydrofuran solvate crystals are reported to undergo desolvation within minutes of being removed from the mother liquor.(Caira *et al.*,

1998) For the three niclosamide crystal forms with known crystals structures, the different modes of solvent inclusion observed correlate well with the desolvation properties observed.(Caira *et al.*, 1998)

In addition to these forms, the structures of four niclosamide cocrystals, with caffeine, urea, *p*-aminobenzoic acid, theophylline, as well as niclosamide theophylline acetonitrile solvate, have been reported.(Sanphui *et al.*, 2012)

In this study, which was part of a broader study of niclosamide solvates and cocrystals in single crystal and bulk form, their hydrogen bonding and properties, we report the preparation of both single crystals and single phase polycrystalline samples of niclosamide methanol solvate (NCL-MeOH), the crystal structure of this solvate, its stability and a description of the solvent inclusion mode in the context of its desolvation properties; we also describe the crystal structure of niclosamide monohydrate H_A and its effect on the stability of this solid form.

2. Experimental

2.1. Single crystal growth

Single crystals of niclosamide methanol solvate were grown from an equimolar mixture of niclosamide (100 mg, 0.31 mmol) and nicotinic acid (36.9 mg, 0.30 mmol) heated in 5 mL MeOH. The solution was separated from solid residue, refluxed for 10 min and cooled to room temperature away from heat. Yellow needles started forming after a couple of hours.

2.2. Polycrystalline material preparation

Niclosamide methanol solvate was prepared by refluxing niclosamide (100 mg, 0.31 mmol) and MeOH (4 mL) for 30 min and cooling to room temperature away from heat. The yellow niclosamide fine powder transformed to yellow microcrystalline material (composed of very fine needles) during this time. Niclosamide hydrate was prepared by the same method, using 100 mg (0.31 mmol) of Niclosamide and 3 mL H_2O. Niclosamide monohydrate H_A was prepared by refluxing NCL (100 mg, 0.31 mmol) and H_2O (3 mL) for 30 min and cooling the product to room temperature.

2.3. Single crystal X-ray diffraction

Single crystal X-ray diffraction data on NCL-MeOH were collected on beamline I19 at Diamond Light Source, using a wavelength of 0.6889 Å and a standard hemisphere data collection (sample to detector distance 60 mm, 2θ detector position 30^o). A needle-shaped crystal of approximate dimensions 0.01 × 0.02 × 0.08 mm^3 was selected for data collection. Data were collected as 2 sec/^{o} exposures. Structure solution and refinement on F^2 were carried out using SIR 92 and CRYSTALS. (Altomare, 1994, Betteridge *et al.*, 2003) Anisotropic atomic displacement parameters (ADPs) were refined for all non-hydrogen atoms. Although the hydrogen atoms could be located in difference Fourier maps, geometric placement was used and the bond lengths and angles regularised. The

hydrogen atoms were then treated using the riding model; the only exception was the hydrogen atom involved in a short O-H…O hydrogen bonds, whose position and isotropic ADP were refined. The Flack parameter could not be refined reliably, so the absolute configuration assignment is arbitrary. Molecular graphics were created using Mercury. (Macrae *et al.*, 2008) All crystallographic details are given in Table 1.

2.4. Powder X-ray diffraction

Powder X-ray diffraction data were collected on a Bruker D8 ADVANCE diffractometer ($CuK_{\alpha 1,2}$ radiation) and a LynxEye detector. Patterns were recorded in ranges between 2 and 60° using a step size of 0.014°. Data analysis was carried out using Topas Academic software.(Coelho *et al.*, 2011).

Table 1 Crystallographic details for NCL-MeOH.

Crystal data	
Chemical formula	$C_{13}H_8Cl_2N_2O_4{\cdot}CH_4O$
M_r	359.16
Crystal system, space group	Orthorhombic, $P2_12_12_1$
Temperature (K)	100
a, *b*, *c* (Å)	3.740 (8), 17.42 (4), 22.18 (5)
V (Å^3)	1445 (6)
Z	4
Radiation type	synchrotron, λ = 0.68890 Å
μ (mm^{-1})	0.43
Crystal size (mm)	0.08 × 0.02 × 0.01
Data collection	
Diffractometer	CrystalLogic diffractometer
Absorption correction	Multi-scan
No. of measured, independent and observed [$I > 2.0\sigma(I)$] reflections	7663, 3252, 2582
R_{int}	0.070
$(\sin\theta/\lambda)_{max}$ (Å^{-1})	0.651
Refinement	
$R[F^2 > 2\sigma(F^2)]$, $wR(F^2)$, *S*	0.095, 0.103, 1.20
No. of reflections	2582
No. of parameters	212
No. of restraints	0
H-atom treatment	Mix of independent and constrained refinement
$\Delta\rho_{max}$, $\Delta\rho_{min}$ (e Å^{-3})	0.48, −0.71

3. Results and discussion

3.1. Niclosamide methanol solvate

NCL-MeOH solvate crystallises in the orthorhombic space group $P2_12_12_1$ with with one NCL and one MeOH molecule in the asymmetric unit (Fig. 2a). The NCL molecule is essentially planar, with the nitro group oxygen atoms having the largest deviation from the mean plane, 0.06 and – 0.07 Å, respectively. Being in the so-called *β*-conformation (Koshelev.Li & Bekhli, 1974), the molecule contains an intramolecular N4-H41···O14 hydrogen bond with a donor-to-acceptor distance of 2.588(9) Å. This geometry is similar to that found in the structure of pure niclosamide (d_{NO} = 2.63 Å).(Sanphui *et al.*, 2012) Each MeOH molecule forms hydrogen bonds to the NCL hydroxyl groups *via* O14-H141···O22 interactions, with d_{OO} = 2.520(9) Å. This hydrogen atom was the only one whose fractional coordinates were refined, and the resulting O14-H141 distance is 0.98(6) Å, reflecting a small degree of proton transfer towards the acceptor in this short O-H···O hydrogen bond.

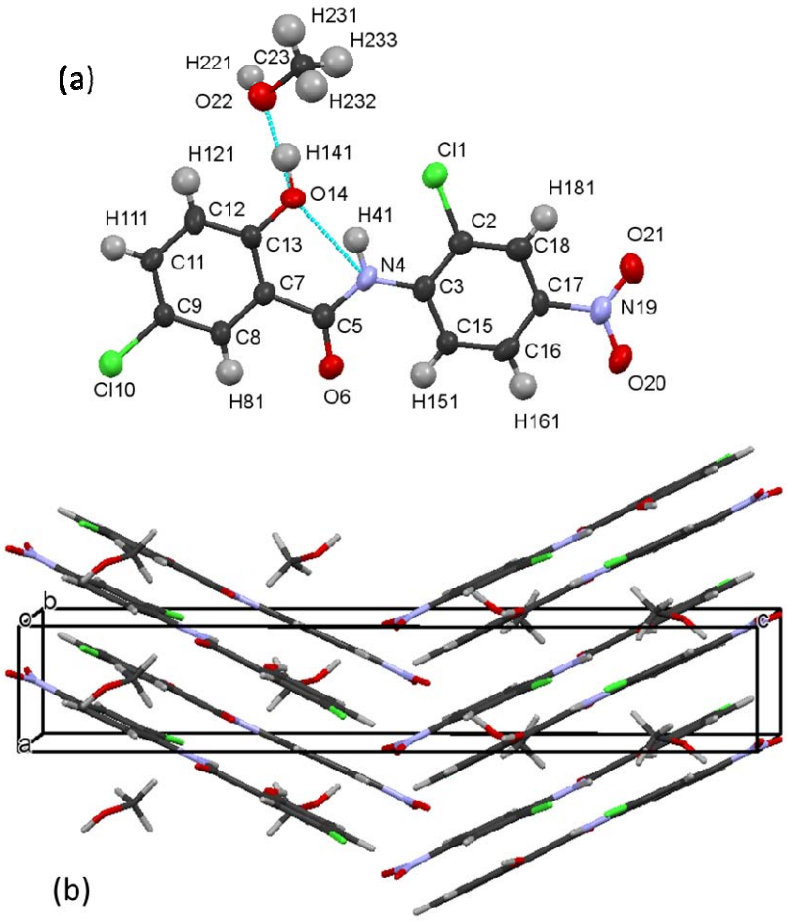

Figure 2 (a) The asymmetric unit of NCL-MeOH with atom numbering. ADPs are drawn at the 50% probability level. (b) Crystal packing in NCL-MeOH.

The Cl···NO_2 interaction with d_{ClO} = 3.215(5) Å between Cl10 and O21 is comparable to that found in guest-free niclosamide (3.22 Å). (Sanphui *et al.*, 2012) Finally, π-π interactions lead to the NCL molecules stacking along the crystallographic *a*-axis and forming a herringbone motif (Fig. 2b). The distance between the planes of the π-π stacked layers is 3.36 Å, comparable to that in pure niclosamide and some of its cocrystals, with the ring centroids 3.740(8) Å apart (the standard uncertainty corresponds to the *a*-unit cell edge). For example, in pure niclosamide, the smallest perpendicular separation between the planes of the stacked layers is 3.34 Å; in the cocrystals with caffeine, urea and *p*-aminobenzoic acid, this separation is 3.32 Å, 3.34 Å and 3.38 Å, respectively. (Sanphui *et al.*, 2012) The MeOH molecules are found to reside in channels along the *a*-axis formed in the host NCL framework, as illustrated in the packing and space-fill diagrams in Fig. 3. The Kitaigorodskii packing index for this structure is 73.9%, and it decreases to 65.4% when the MeOH molecules are removed.

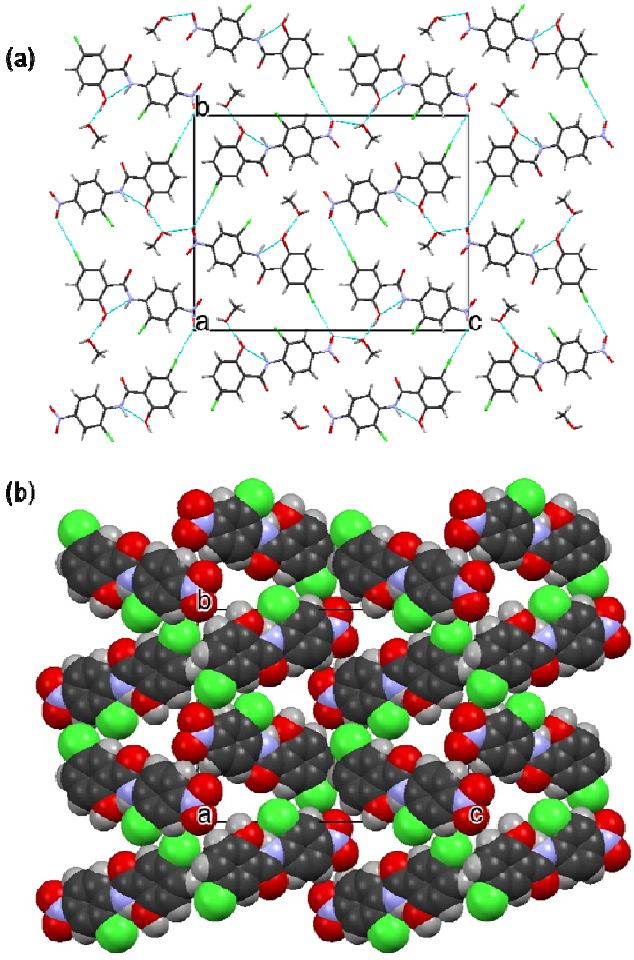

Figure 3 Location of the MeOH molecules in the NCL host framework. (a) Crystal packing in NCL-MeOH viewed in the (*bc*) plane; the highlighted interactions are discussed in the text. (b) Space-fill diagram showing continuous channels in the *a*-direction (guest molecules deleted for clarity).

Refluxing niclosamide in methanol for 30 minutes yielded a microcrystalline yellow product, identified by PXRD as single phase NCL-MeOH solvate. Fig. 4a shows the Pawley fit (Pawley, 1981) to the pattern recorded on the material while still wet (R_{wp} = 6.14%). Pawley fitting was used for PXRD data analysis rather than the Rietveld method because of the severe preferred orientation arising from placing a wet microcrystalline powder consisting of needle-shaped crystals on a flat plate sample holder. No peaks are unaccounted for, demonstrating unambiguosly the phase purity of the product. Fig. 4b shows the fit to the PXRD pattern recorded on the sample after it was stored in air overnight (R_{wp} = 4.17%). Although the NCL-MeOH solvate is still the majority phase, extra peaks (marked in Fig. 4b) have appeared which indicate the presence of niclosamide hydrate (*vide infra*). The instability of NCL-MeOH relative to the hydrate demonstrated here by PXRD is consistent with the conclusions from thermal analysis measurements reported by van Tonder *et al*. (van Tonder, Mahlatji*, et al.*, 2004)

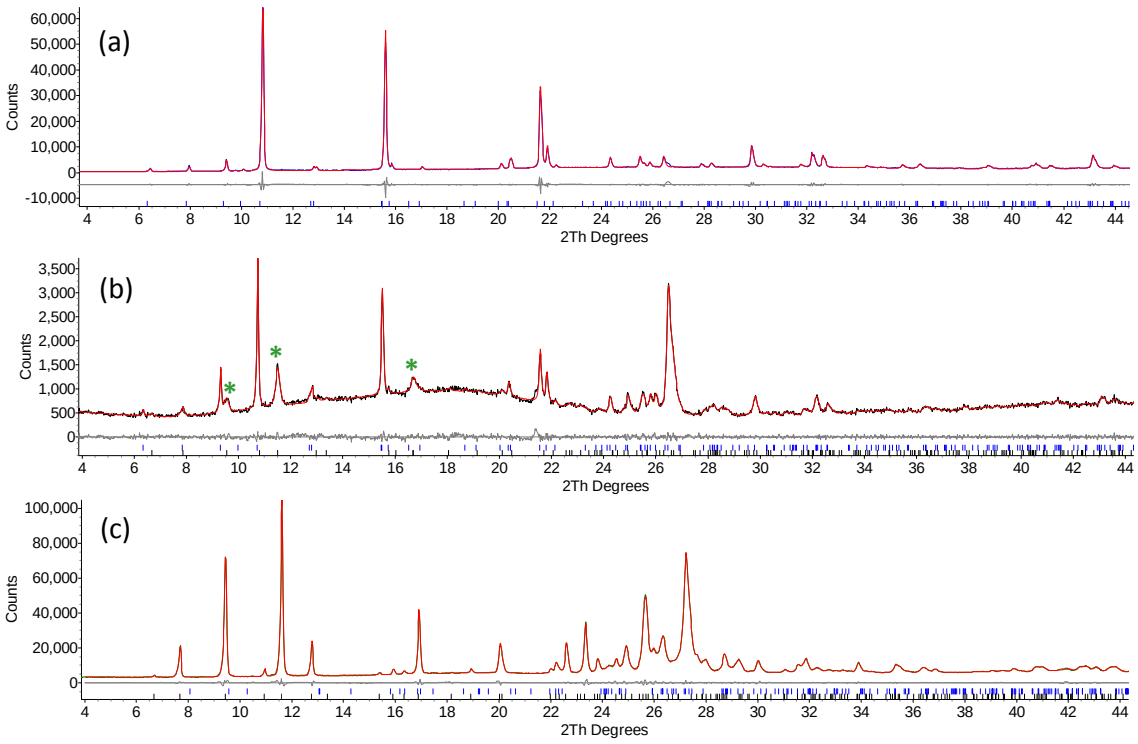

Figure 4 PXRD patterns of NCL-MeOH and NCL hydrate samples made by reflux. (a) Pawley fit to the NCL-MeOH pattern obtained on the wet product; (b) Pawley fit to the PXRD pattern of NCL-MeOH collected after storing in air overnight; (c) Pawley fit to the PXRD pattern of NCL monohydrate H_A (black tick marks), with a small amount of monohydrate H_B (blue tick marks).

3.2. Niclosamide monohydrate H_A

The diffraction pattern of the freshly prepared NCL monohydrate H_A (Fig. 4c) was indexed using the positions of 20 reflections up to 25° 2θ. (Coelho, 2003) The obtained unit cell and space group $P2_1/c$ were used to carry out a Pawley fit to the observed data set, and the final refined unit cell was a = 3.8590(2) Å, b = 16.1578(6) Å, c = 23.047(1) Å, β = 91.60(2)° and V = 1436.4(1) Å^3. This left a few discrepancies in the fit in the 2θ range between 22 and 30 degrees, which could be accounted for by the presence of a small amount of monohydrate H_B, as shown by the two-phase fit depicted in Fig. 4c (R_{wp} = 2.84%). The unit cell parameters obtained for monohydrate H_B were a = 11.10(2) Å, b = 17.20(3) Å, c = 7.476(7) Å, β = 99.29(6)° and V = 1408(4) Å^3. This unit cell volume is smaller than that of H_A, which is consistent with the relative stabilities of the two monohydrates.

The similarity of the unit cell parameters of monohydrate H_A and NCL-MeOH suggests that these two crystal forms may be essentially isostructural, possessing a very similar packing arrangement of niclosamide molecules and very similar cavities in which the solvent molecules reside, although this is not possible to demonstrate beyond the Pawley fit, through Rietveld refinement of the structure, due to the severity of the preferred orientation and the complexity of the structure relative to the data quality. However, the following factors support the proposed relationship between the NCl-MeOH solvate and monohydrate H_A. The unit cell found for the latter gives an essentially flawless Pawley fit and has a logical relationship to the size of the unit cell of H_B. Secondly, isostructural methanol solvates and hydrates are known to exist. (Clarke *et al.*, 2012) Finally, monohydrate H_A adopting the proposed structure, such that the water molecules reside in continuous channels along the *a*-direction, correlates very well with the observed onset of dehydration at 102°C, significantly below the dehydration temperature of H_B.

4. Implications of the structure for properties

Desolvation temperatures determined by differential scanning calorimetry for niclosamide monohydrates H_A and H_B, and the MeOH, tetrahydrofuran (THF) and tetraethylene glycol (TEG) solvates have been reported as 102°C, 174°C/199°C (two-step process), 90 ± 3°C, 75 ± 10°C and 103 ± 5°C, respectively.(van Tonder, Mahlatji*, et al.*, 2004, van Tonder, Maleka*, et al.*, 2004) The exceptionally high dehydration onset temperature in the monohydrate H_B is explained by the fact that in this crystal structure water molecules are found as pairs confined in cavities formed by the NCL molecules. The crystal packing in the THF and TEG solvates is markedly different; solvent molecules are located in continuous channels and in layers alternating with layers of NCL molecules, respectively.(Caira *et al.*, 1998) The topology of the NCL-MeOH solvate and monohydrate H_A, described above and depicted in Fig. 3, is similar to that of the THF solvate, with the channels along the crystallographic *a*-axis providing pathways for the diffusion of solvent/water molecules out from

the crystal, resulting in relatively low desolvation/dehydration temperatures of these solid forms, comparable to those of NCL-THF and NCL-TEG solvates.

Given that the NCL-MeOH solvate and monohydrate H_A are isostructural, it is not surprising that the former readily transforms into the latter when stored at ambient conditions. The PXRD data shown in Fig. 4 demonstrate that this solvent molecule exchange transformation occurs in air on a time-scale of several hours.

5. Conclusions

The structure determination of NCL-MeOH solvate, performed using single crystal synchrotron X-ray diffraction on small needle-shaped crystals grown by reflux, elucidated the key non-covalent interactions. The essentially planar niclosamide host molecules form a herringbone-type packing arrangement, facilitated by π-stacking. There are channels along the crystallographic *a*-axis in which the methanol guest molecules are located. The methanol guest and niclosamide host molecules interact via O-H···O hydrogen bonds. Powder X-ray diffraction reveals that initially phase-pure niclosamide methanol solvate readily transforms into niclosamide monohydrate at ambient conditions.

Indexing and Pawley fitting of the PXRD pattern of niclosamide monohydrate H_A suggest that this solid form is isostructural with the NCL-MeOH solvate. This structural insight is consistent with the low dehydration temperature of H_A relative to monohydrate H_B and with the transformation of the methanol solvate into hydrate when stored in air.

The topology and the guest molecule inclusion mode in NCL-MeOH and monohydrate H_A allow us to correlate their relatively low desolvation temperature with the crystal structure; the continuous channels in which the MeOH and water molecules reside provide pathways for their removal from the material. Our crystallographic results thus give insights into the host-guest interactions in NCL-MeOH which correlate well with the structure – property relationships of the other niclosamide solvates with known crystal structures.

References

Altomare, A. C., G.; Giacovazzo, A.; Guagliardi, A.; Burla, M.C.; Polidori, G.; Camalli, M (1994). *Journal of Applied Crystallography* **27**, 437.

Betteridge, P. W., Carruthers, J. R., Cooper, R. I., Prout, K. & Watkin, D. J. (2003). *Journal of Applied Crystallography* **36**, 1487.

Caira, M. R., Van Tonder, E. C., De Villiers, M. M. & Lotter, A. P. (1998). *Journal of Inclusion Phenomena and Molecular Recognition in Chemistry* **31**, 1-16.

Clarke, H. D., Hickey, M. B., Moulton, B., Perman, J. A., Peterson, M. L., Wojtas, L., Almarsson, O. & Zaworotko, M. J. (2012). *Crystal Growth & Design* **12**, 4194-4201.

Coelho, A. A. (2003). *Journal of Applied Crystallography* **36**, 86-95.

Coelho, A. A., Evans, J. S. O., Evans, I. R., Kern, A. & Parsons, S. (2011). *Powder Diffraction* **26**, S22.

Helfman, D. M. (2011). *Journal of the National Cancer Institute* **103**, 991-992.

Imperi, F., Massai, F., Pillai, C. R., Longo, F., Zennaro, E., Rampioni, G., Visca, P. & Leoni, L. (2013). *Antimicrobial Agents and Chemotherapy* **57**, 996-1005.

Koshelev.Li & Bekhli, A. F. (1974). *Khimiko-Farmatsevticheskii Zhurnal* **8**, 57-60.

Macrae, C. F., Bruno, I. J., Chisholm, J. A., Edgington, P. R., McCabe, P., Pidcock, E., Rodriguez-Monge, L., Taylor, R., van de Streek, J. & Wood, P. A. (2008). *Journal of Applied Crystallography* **41**, 466-470.

Manek, R. V. & Kolling, W. M. (2004). *AAPS PharmSciTech* **5**, E14-E14.

Pawley, G. S. (1981). *Journal of Applied Crystallography* **14**, 357.

Sanphui, P., Kumar, S. S. & Nangia, A. (2012). *Crystal Growth & Design* **12**, 4588-4599.

Steiner, T. (2002). *Angewandte Chemie-International Edition* **41**, 48-76.

Tian, F., Qu, H., Louhi-Kultanen, M. & Rantanen, J. (2010). *Chemical Engineering & Technology* **33**, 833-838.

van Tonder, E. C., Mahlatji, M. D., Malan, S. F., Liebenberg, W., Caira, M. R., Song, M. N. & de Villiers, M. M. (2004). *Aaps Pharmscitech* **5**.

van Tonder, E. C., Maleka, T. S. P., Liebenberg, W., Song, M. N., Wurster, D. E. & de Villiers, M. M. (2004). *International Journal of Pharmaceutics* **269**, 417-432.

Weinbach, E. C. & Garbus, J. (1969). *Nature* **221**, 1016-1018.

Yo, Y. T., Lin, Y. W., Wang, Y. C., Balch, C., Huang, R. L., Chan, M. W. Y., Sytwu, H. K., Chen, C. K., Chang, C. C., Nephew, K. P., Huang, T., Yu, M. H. & Lai, H. C. (2012). *Molecular Cancer Therapeutics* **11**, 1703-1712.